Structures from the Melt," (ibid.), 603-650; J. H. Westbrook, "The Sources of Strength and Brittleness in Intermetallic Compounds," (ibid.), 724-768; D.C. Drucker, "Engineering and Continuum Aspects of High Strength Materials," (ibid.), 795-833.

3. N. I. Tymiak, D. E. Kramer, D. F. Bahr and W. W. Gerberich, "Plastic Strain Gradients at Very Small Penetration Depths," Acta Mater. 49 (2001), 1021-1034.

4. W. W. Gerberich, N. I. Tymiak, J. C. Grunlan, M. F. Horstemeyer and M. I. Baskes, "Interpretations of Indentation Size Effects," J. Appl. Mech. 62 (2002), 433-442.

5. M. Baskes and M. Horstemeyer, private communication, Sandia National Labs, Livermore, CA (1999).

6. W. W. Gerberich, J. M. Jungk, M. Li, A. A. Volinsky, J. W. Hoehn and K. Yoder, "Length Scales for the Fracture of Nano-structures," Intern. J. of Fracture (2003), accepted.

7. W. W. Gerberich, W. M. Mook, C.R. Perrey, C. B. Carter, M. I. Baskes, R. Mukherjee, A. Gidwani, J. Heberlein, P. H. McMurray and S. L. Girshick, "Superhard Silicon Nanospheres," J. Mech. Phys. Solids (2003), in press.

8. F. DiFonzo, A. Gidwani, M. H. Fan, D. Neumann, D. J. Iordanoglu, J. V. R. Heberlein, P. H. McMurry, S. L. Girshick, N. Tymiak, W. W. Gerberich and N. P. Rao, Appl. Phys. Lett. 77 (2000), 910-912.

9. D. E. Kramer, H. Huang, M. Kriese, J. Robach, J. Nelson, A. Wright, D. Bahr and W. W. Gerberich, "Yield Strength Predictions from the Plastic Zone around Nanocontacts," Acta Mater. 47 (1994), 333-343.

10. J. P. Hirth and J. Loethe, Theory of Dislocations, 2nd ed. (New York, NY: John Wiley and Sons, 1982).

11. J. M. Jungk, W. M. Mook and W. W. Gerberich, "Nanoindentation Length Scale Measures in Small Volumes," in preparation.

Nano and Microstructural Design of Advanced Materials
M.A. Meyers, R.O. Ritchie and M. Sarikaya (Editors)
© 2003 Elsevier Ltd. All rights reserved.

THE ONSET OF TWINNING IN PLASTIC DEFORMATION AND MARTENSITIC TRANSFORMATIONS

Marc André Meyers[1], Matthew S. Schneider[1], and Otmar Voehringer[2]

[1]University of California-San Diego, Dept. of MAE, La Jolla, CA 92093 USA
[2]University of Karlsruhe, Inst. for Matls. Research., Karlsruhe Germany

ABSTRACT

A quantitative constitutive description for the criterion postulated by Thomas [1-3] for the morphology of martensitic transformations is presented. Thomas observed that the temperature and strain-rate sensitivities of slip are much higher than those for twinning, rendering twinning a favored deformation mechanism at low temperatures and high strain rates. Constitutive relationships for slip and twinning are presented and applied to the martensitic transformation in steels: the lath to plate morphology change that is observed with increasing carbon content is successfully predicted by calculations incorporating the two modes of deformation. The Hall-Petch coefficient, for the inclusion of grain size effects is two times larger for twinning than slip. A simple calculation of the strain rates during martensitic transformation is also provided.

For FCC metals, the constitutive description for the slip-twinning transition incorporates the effects of material (stacking-fault energy, grain size, composition) as well as external (temperature, strain rate) parameters successfully. It can also applied to the shock compression regime, where the shock front thickness (and, consequently, strain rate) is related to the peak pressure by the Swegle-Grady relationship. Predictions are compared to seminal shock loading work by Johari and Thomas [4] and Nolder and Thomas [5] demonstrating that there is a threshold pressure for twinning in copper and nickel.

INTRODUCTION

It was shown by Thomas [1-3] that slip and twinning are competing deformation mechanisms and that they have a profound effect on the mechanical properties of martensitic steels and FCC metals like copper and nickel. The schematic representation by Thomas [2] is shown in Figure 1. This plot, although qualitative, provides deep insight into the mechanical response of metals and alloys, which can deform by slip, twinning, or martensitic transformations. Figure 1 shows that slip has substantially higher temperature dependence than twinning; hence, slip and twinning domains are established. Martensitic transformations are displacive, virtually diffusionless transformations with the thermodynamics and kinetics governed by the transformation strains. In steels, the martensite structure undergoes a drastic morphological transition as the carbon content reaches the 0.6-1.0 weight percent region. Early German literature classified the two regions into *Schiebung* and *Umklapp;* the current nomenclature is *lath* and *plate* where the basic difference resides in the deformation mode: the transition from slipped (lath) to twinned (plate) martensite. Figure 2 shows the change in Ms as well as the two modes as a function of increasing carbon content [6]. Figure 3 shows transmission electron micrographs of the two morphologies in different compositions of steel. This paper provides a quantitative description of the transition from

lath to plate martensite by applying the Zerrilli-Armstrong constitutive equation. It is a straightforward method of predicting the threshold carbon concentration for the nucleation of plate martensite as a function of strain rate, temperature, and grain size.

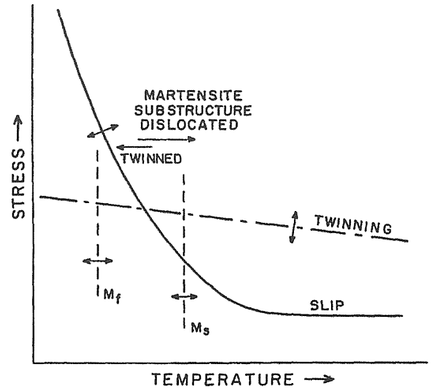

Figure 1: Variation of the stress for slip and twinning as a function of temperature. Composition variations are expected to affect the slip-twin cross-over as suggested by the arrows. (Adapted from Thomas [2]).

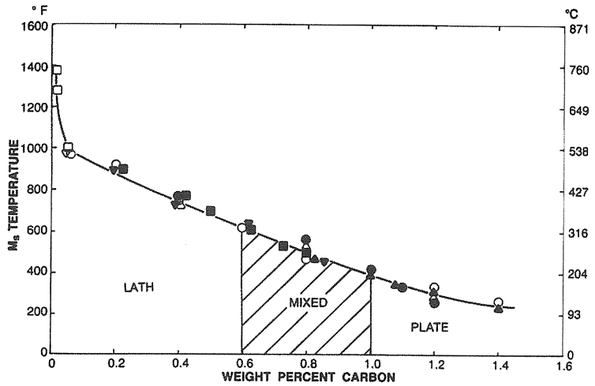

Figure 2: Variation of Ms temperature with carbon content; notice transition from lath (slipped) to plate (twinned) morphology; from Marder and Krauss[11].

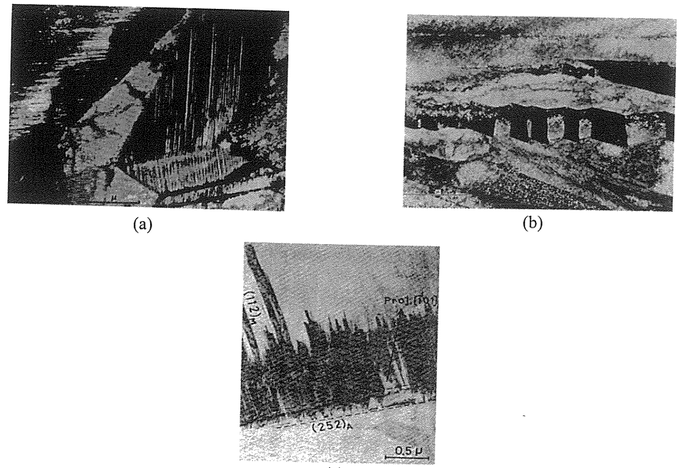

Figure 3: (a) Twinned plates of martensite and residual austenite in Fe-33Cr-.01C; (b) Twinned and dislocated martensite in Fe-28Ni-01C; (c) Twinned plates of martensite in Fe-8Cr-1C; from Thomas [3].

CALCULATIONAL PROCEDURE

The calculations require constitutive equations for slip and twinning that have the appropriate temperature and strain rate dependencies. These equations were implemented by Meyers et al. [7,8] into a slip-twinning transition criterion and will only be briefly described herein By considering slip and twinning as competing mechanisms, and equating the appropriate constitutive equations, one obtains the critical condition:

$$\sigma_T = \sigma_S \tag{1}$$

where σ_S and σ_T are the slip and twinning stresses, respectively.

Constitutive Description of Slip

There are numerous equations that successfully incorporate the strain, strain rate and temperature effects and predict the mechanical response over a broad range of external parameters. The Zerilli-Armstrong [9] equation is used here to describe the lath to plate transition in martensite. It is modified to incorporate the solid solution hardening effects induced by carbon additions. There are two different forms of the equation applicable to FCC and BCC metals. The barrier size is quite different: dislocation forest dislocations are considered the primary barriers for FCC materials, whereas the Peierls-Nabarro stress is the principal obstacle for BCC materials. These differences are responsible for higher strain rate and temperature sensitivity for the BCC structure. When iron-based alloys undergo the martensitic transformation, the FCC structure transforms to BCC or BCT. This newly created structure has to undergo a complex deformation to accommodate the Bain and lattice invariant strains. The Zerilli-Armstrong equation for the BCC structure has the form:

$$\sigma = C_s * \exp[T*(-C_t + C_r * \ln(\dot{\varepsilon}))] + C_h * \varepsilon^{C_n} + \sigma_g + \sigma_c \quad (2)$$

The variables are strain, ε, strain rate, $\dot{\varepsilon}$ and temperature, T. The coefficients C_s, C_t, Cr, C_h, and C_n are experimentally obtained parameters. The parameters, their physical meanings and values chosen are for pure iron [9]:

C_S: Stress Constant	1033 MPa
C_t : Thermal Softening Constant	0.00698
C_r : Strain Rate Constant	0.000415
C_h: Strain Hardening Constant	266 MPa
C_n: Strain Hardening Constant	0.289

The terms σ_g and σ_c represent the athermal components of stress, which have minimal strain rate and temperature dependence. The grain size term, σ_g represents the grain-size dependence, which is represented by a Hall-Petch relationship:

$$\sigma_g = k_s d^{-1/2} \quad (3)$$

where k_S for low carbon steels is found to vary between 15-18 MPa/mm$^{1/2}$ [10]. An average value of 16.5 MPa/mm$^{1/2}$ is used in the calculations. Figure 4 shows the Hall-Petch plots for both slip and twinning. The value matches well with experimental data by Marder and Krauss [11].

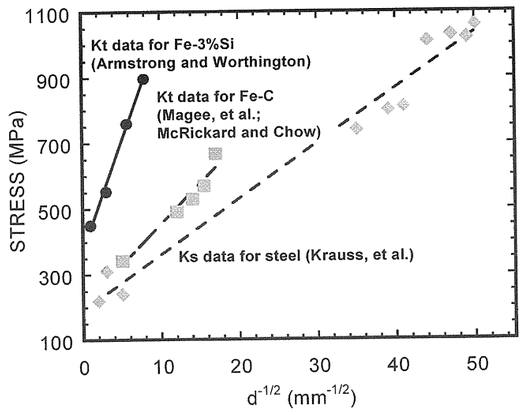

Figure 4: Effect of grain size on stress for slip (k_s) and twinning (k_t).

σ_c represents the contribution to strength due to the presence of solute atoms (in this case, carbon). It is observed that the flow stress at large concentrations of solute varies with the square root of carbon content [12]:

$$\sigma_c = k\,[\text{carbon}]^n \quad (4)$$

n is often given as 0.5 and for this case k is 450 MPa. For lower concentrations, Pickering and Gladman [13] use a linear fit to describe the solid solution hardening effect of carbon in austenite with a coefficient of 324 MPa/wt% carbon.

Figure 5 shows the predicted stress-strain curves for different (a) grain sizes; (b) carbon contents; (c) strain rates; and (d) temperatures. The calculated curves agree well with experimentally-obtained curves.

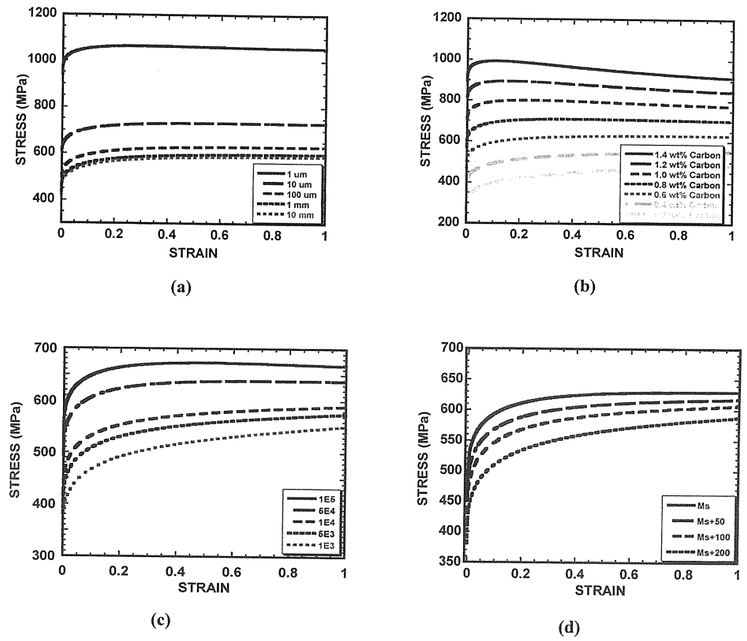

Figure 5: Calculated stress-strain curves (assuming slip) for different: (a) grain sizes; (b) carbon contents (D=100 μm; strain rate=10^4 s^{-1}); (c)strain rates; (d) temperatures above M_s.

Constitutive Equation for Twinning

In these calculations, the twinning stress is assumed to be relatively independent of strain, temperature, and strain rate, in contrast to slip processes and therefore no work hardening effects are taken into account. Nevertheless, the grain-size dependence is much larger. Indeed, k_T values are 2-4X greater than k_S values. The following equation was used:

$$\sigma_T = \sigma_O + k_T d^{-1/2} \tag{5}$$

Armstrong and Worthington [14] report for Fe-3%Si: k_T=66.3 MPa/mm$^{1/2}$. For low-carbon iron, McRickard and Chow [15] and Magee et al. [16] report values of 45.5 MPa/mm$^{1/2}$. This latter value is used here. Figure 6 shows the experimental results by Magee et al. [16] as well as the best-fit plot for the effect of carbon on the twinning stress of steel:

$$\sigma = 662 \text{ MPa} * [\text{at\%C}]^{0.158} \tag{6}$$

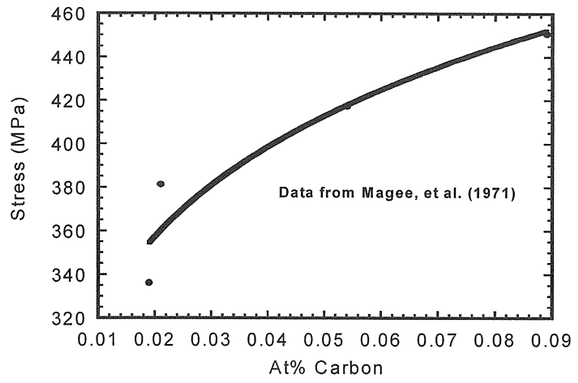

Figure 6: Effect of interstitial carbon on the twinning stress of iron-carbon alloy (from Magee et al. [16]).

The twinning stresses are extrapolated from this curve for higher concentrations of carbon. Figure 7 shows the predicted stress-strain curves for different (a) grain sizes and (b) carbon contents.

Martensitic Strains and Strain Rates:

Figure 8 shows, in a schematic fashion, the growth of martensite lens. The material within the expanding lens is subjected to Bain and lattice invariant strains.

During martensitic transformations, the strain rate can be approximated by:

$$\dot{\gamma} = \frac{\gamma}{t} \approx \frac{\gamma \nu}{D} \tag{7}$$

where ν is the growth velocity for the martensite lens, γ is the transformation strain (γ = 0.2) and D is the grain diameter. In Figure 8, two growth directions are indicated: longitudinal and transverse growth.

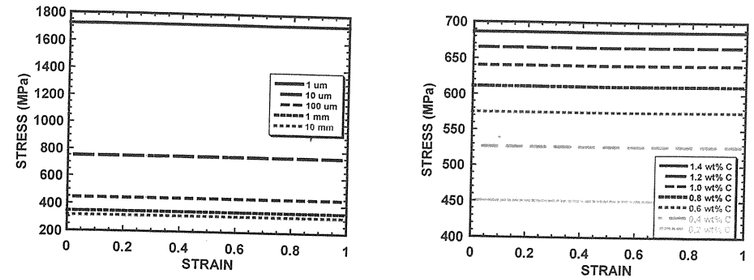

Figure 7: Room-temperature stress-strain curves assuming twinning for different grain sizes and carbon contents.

Meyers [17] has analyzed the two modes and discusses the two velocities. The longitudinal growth velocity has been measured by Bunshah and Mehl [18] for Fe-Ni-C alloys; it was found to be equal to 1,00m/s. Schoen and Owen [19] measured the lateral growth velocity for Fe-10Ni-C alloys with carbon contents between 0 and 0.010. The values varied from 0.01 to 1 m/s. Considering a range of velocities of 1-1000 m/s, one obtains a range of strain rates:

$$\dot{\gamma} = \frac{0.20 * \nu}{D} \approx \frac{1}{D}(0.2 \rightarrow 200) \tag{8}$$

For a grain size of 100 μm (a reasonable value for Fe alloys), this provides the following range of strain rates:

$\dot{\gamma} \approx 2x10^3 \rightarrow 2x10^6 s^{-1}$

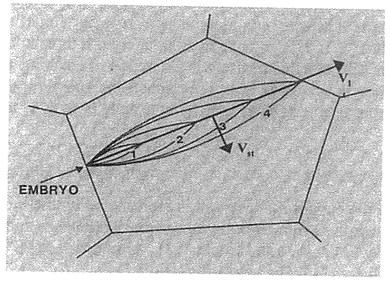

Figure 8: Schematic representation of growth of martensite lens with longitudinal (V_l)

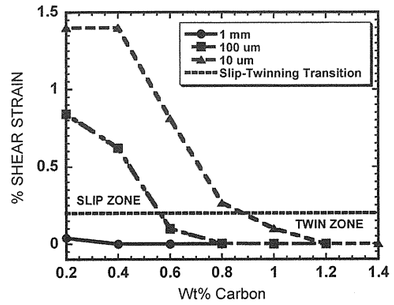

Figure 9: Predicted carbon content for slip-twinning transition in martensitic transformation in steels with different grain sizes a function of carbon content; shear strain for martensitic transformation equal to 0.2..

In the calculations conducted and reported herein, a strain rate of 10^3 $s^{-1}$was assumed. It is interesting to notice that the strain rate along the mid-rib (region subjected to longitudinal growth) the strain rate is much higher. It is also observed that this region is more prone to twinning. Often, one observes martensite lenses with twinning along the mid-rib and dislocations in the lateral growth regions.

The results of the computations are shown in Figure 9. Calculations were conducted for three grain sizes: 10, 100, and 1000 μm. For the 100μm grain size, the predicted transition from dislocated to twinned martensite is in excellent agreement with the observed results: 0.55 wt% C. For the other grain sizes, significant differences are observed. It would be interesting to verify whether the predictions of this simple model are corroborated by experiments: a reduction of grain size favors dislocated (plate) martensite.

PREDICTED VALUES IN SHOCK COMPRESSION

The procedure presented in this section [7,8] can be used to predict the critical pressure for twinning in shock compression experiments. The early experiments performed by Johari and Thomas [4] in Cu and Cu-Al and Nolder and Thomas [5] in Ni demonstrated that there is a threshold pressure for twinning. It has been established by Murr [20] that this pressure is a function of stacking-fault energy for FCC metals. The application of this criterion to the shock front necessitates the knowledge of the strain rate. The strain rate at the shock front has been established by Swegle and Grady [21] to be:

$$P = k_{SG}\,\dot{\varepsilon}^{1/4} \tag{9}$$

The constitutive response of the copper monocrystal is represented by the modified mechanical threshold stress (MTS) expression below; the parameters are taken from Follansbee and Gray [22]. The MTS model and parameters are defined by Follansbee and Kocks [23]. A modified MTS equation is used, with values of p=1/2 and q= 3/2, respectively [24]. The value of g_0 is 0.8 [25].

$$\sigma=\sigma_0 f(\varepsilon)\left[1-\left(\frac{kT}{Gb^3 g_0}\ln\left(\frac{\dot{\varepsilon}_0}{\dot{\varepsilon}}\right)\right)^{2/3}\right]^2+\mathrm{kd}^{-1/2} \tag{10}$$

We apply Eqn. (1) to Eqn. (10), assuming a constant σ_T. We find $\dot{\varepsilon}$ from Eqn. 10, which is inserted into Eqn (9). This provides a first estimate of the pressure, P, where $f(\varepsilon)$ is an experimentally obtained stress-strain relationship (polynomial expression). This pressure is then used to calculate the shock strain and temperature through the Rankine-Hugoniot relations. This procedure is iterative. Figure 8 shows the application of this method to copper. The plot shows how the initial temperature and grain size affect the threshold shock pressure. The calculated threshold pressure for a monocrystal (10 mm grain size) shocked from an initial temperature of 300 K is 17 GPa. This compares favorably with experimental results by De Angelis and Cohen [26]: 14 GPa. Recent laser compression experiments by Meyers et al. [27] yield a threshold stress in this range. Two transmission electron micrographs are shown in Figure 11: copper shocked at (a) 12 GPa (below the twinning threshold) and; (b) copper shocked at 40 GPa (above the twinning threshold).

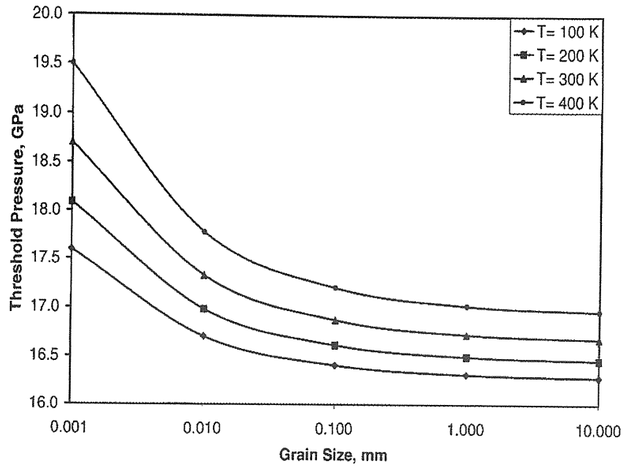

Figure 10: Calculated threshold stress for twinning in shock compression of monocrystalline copper (from Meyers et al. [8]).

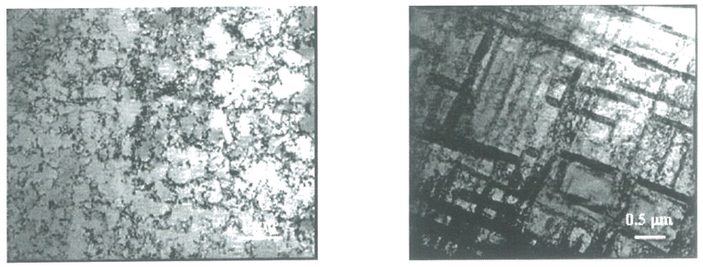

(a) (b)

Figure 11: Laser shocked monocrystalline copper at (a) 12 GPa (below the twinning threshold) and; (b) 4 GPa (above the twinning threshold.

CONCLUSIONS

- The slip-twinning transition criterion postulated by Thomas [1-3] and recently quantified by Meyers et al. [7,8] is applied to martensitic transformation.
- The constitutive response by slip is described by Zerilli-Armstrong equation with addition of interstitial strengthening term. A simple non-work hardening twinning equation was used.
- The model predicts change from lath to plate as carbon content exceeds 0.56 wt%, at a grain size of 100 μm. This is in agreement with experiments. It is interesting to notice that the predicted change in lath to plate morphology is dependent on the austenitic grain size.
- By the application of the Swegle-Grady relationship to the slip-twinning criterion, it is possible to extend the prediction to threshold pressure in shock compression. Johari and Thomas [5] observed a slip-twinning transition in shock compressed copper which was successfully calculated through the constitutive approach outlined here.
- It is therefore concluded that the Thomas criterion is successfully quantified.

REFERENCES

1. Thomas, G. (1965) *Acta Met.* **13**, 1211.
2. Thomas, G. (1971) *Met. Trans.* **2**, 2373.
3. Johari, O. and Thomas, G. (1965) *Trans. ASM*, **58**, 563.
4. Johari, O. and Thomas, G., (1964) *Acta Mat*, **12**, 1153.
5. Nolder, and Thomas, G., (1964) *Acta Met.,* **12**, 227.
6. Krauss, G. (1980) Principles of Heat Treatment of Steel, ASM, Metals Park, OH, p. 52.
7. Meyers, M. A., Voehringer, O, and Chen, Y. J., in *Advances in Twinning*, eds. S. Ankem and C. S. Pande, TMS,1999, pp. 43-66.
8. Meyers, M. A., Voehringer, O., and Lubarda, V., (2001) *Acta Mat*, **49**, 4025.
9. Zerilli, F.J., and Armstrong, R.W., (1987) *J. Appl. Phys.*, **61**, 1816.
10. Pickering, F. B. *Constitution and Properties of Steels, Materials Science and Technology 7*, VCH Publishing, NY,1992.
11. Marder, A.R., and Krauss, G., *Proc. on the Strength of Metals and Alloys*, Vol 3, ASM, Metals Park, OH, 1970, pp. 822-823.

12. Pickering, F. B. *Physical Metallurgy and the Design of Steels*, Applied Science Publishers, Essex, England, 1978.
13. Pickering, F.B. and Gladman, T. (1963) *T. Iron and Steel Inst. Spec. Rep. #81*, **10.**
14. Armstrong, R. W., and Worthington, P. J., (1974) in *Metallurgical Effects at High Strain Rates,* eds. R. Rohde, B. Butcher, J. Holland, and C. Karnes. Plenum, NY, p. 41.
15. McRickard, S. B., and Chow, J. G. Y., (1965) *Trans. AIME*, **223**, 147.
16. Magee, C.L., Hoffman, D.W. and Davies, R.G., (1971) *Phil. Mag*. **23**, 1531.
17. Meyers, M. A., (1979) *Acta Met*., **28**, 757.
18. Bunshah, R. F., and Mehl, R. F., (1953) *J. Metals*, **5**, 1251.
19. Schoen, F. J., and Owen, W. S., (1971) *Met. Trans*., **2**, 2431.
20. Murr, L. E., (1988) in *Shock Waves in Condensed Matter*, Eds. Schmidt, S. C. and Holmes, N. C., Elsevier, Amsterdam, pp. 315.
21. Swegle,W and Grady, D. E., (1983) *J. Appl. Phys*., **58,** 941.
22. Follansbee, P. S. and Gray III, G. T., (1991) *Matls. Sci. and Eng*. **138,** 23.
23. Follansbee, P. S. and Kocks, U. F., (1988) *Acta Met.,* **36**, 81.
24. Follansbee, P.S., in *Metallurgical Applications of Shock –Wave and High-Strain Rate Phenomena* ed, L. E. Murr, K. P. Staudhammer, and M. A. Meyers, M. Dekker. 1986, pp.451.
25. Gray III, G.T., in "Shock-Wave and High-Strain-Rate Phenomena in Materials", eds. M.A. Meyers, L.E. Murr, and K.P. Staudhammer, M. Dekker, NY, 1992, pp. 899.
26. De Angelis, R.J, and Cohen, J. B. (1963) *J. of Metals*, **15,** 681.
27. Meyers, M.A. Gregori, F., Kad, B., Schneider, M.S., Remington, B., Kalantar, D., Boehly, T., Ravichandran, G, and Wark, J. (2003) *Acta Mat*. **51**, 1211.